ORNL
MASTER COPY
DATE ISSUED JAN 07 1986

OAK RIDGE NATIONAL LABORATORY

OPERATED BY MARTIN MARIETTA ENERGY SYSTEMS, INC.
POST OFFICE BOX X, OAK RIDGE, TENNESSEE 37831

[redacted]

ORNL
CENTRAL FILES NUMBER
ORNL/CF-85/345

DATE: December 2, 1985

SUBJECT: NATC - A Simple Model for Analysis of Single-Phase, Water Cooled, Natural Convection Systems

TO: Distribution

FROM: S. R. Greene

ABSTRACT

This document describes a simple mathematical model (named NATC) which has been developed for investigation of natural circulation phenomena in heated, single-phase, water cooled loop systems. Results of a benchmark study in which NATC predictions were compared to data from an experiment recently performed at the Tennessee Valley Authority's Engineering Laboratory are presented. The NATC modeling topology is described and user input requirements are discussed.

[redacted]

CONTENT

Page

1. INTRODUCTION..... 1

2. MODEL DERIVATION AND IMPLEMENTATION..... 2

2.1 Model Derivation.....2
2.2 Model Implementation.....6

3. BENCHMARK STUDY: TVA THERMAL PUMP EXPERIMENT..... 8

3.1 Description of Experiment.....8
3.2 NATC Analysis of Experiment.....10

4. CONCLUSIONS.....22

REFERENCES.....24

APPENDIX A: NATC Input Data Description.....34

APPENDIX B: NATC Thermal Pump Model Input
Data Provided by TVA 38

APPENDIX C: Example NATC Input Data File.....41

1. INTRODUCTION

This document describes a simple mathematical model (named NATC) which has been developed for investigation of natural circulation phenomena in heated, single phase, water-cooled loop systems. Results of a benchmark study in which NATC predictions were compared to data from an experiment recently performed at the Tennessee Valley Authority's Engineering Laboratory are presented. The NATC modeling topology is described and user input requirements are discussed.

2. MODEL DERIVATION AND IMPLEMENTATION

2.1 Model Derivation

Figure 1 is a pictorial representation of simple, closed piping loop, consisting of a heated section (with the heater initially turned off), a riser section, and a downcomer/return section. The loop is filled with water which is assumed to be at thermal equilibrium with its surroundings. Given these conditions, there will be no bulk circulation of the fluid through the loop. If, however, the heater is turned on, the resulting water temperature increase in the heated section will produce density head differences in the two vertical columns of the loop-eventually leading to bulk circulation of fluid through the loop. One desires to calculate (a) the time dependent induced loop flow rate, and (b) the time and space dependent loop fluid temperatures.

Lewis (Ref. 1) has presented an analysis of a similar situation, which will be closely followed in the derivation presented here. The loop flow equation is derived from the familiar loop pressure balance considerations:

$$DP\ (total) = DP\ (core) + DP\ (riser) + DP\ (return) = 0 \qquad \text{(Eq. 1)}$$

where

DP (total) = integrated loop pressure drop

DP (core) = total core pressure drop from core inlet to outlet

DP (riser) = total riser pressure drop from riser inlet to riser outlet

DP (return) = total downcomer pressure drop from downcomer inlet to outlet

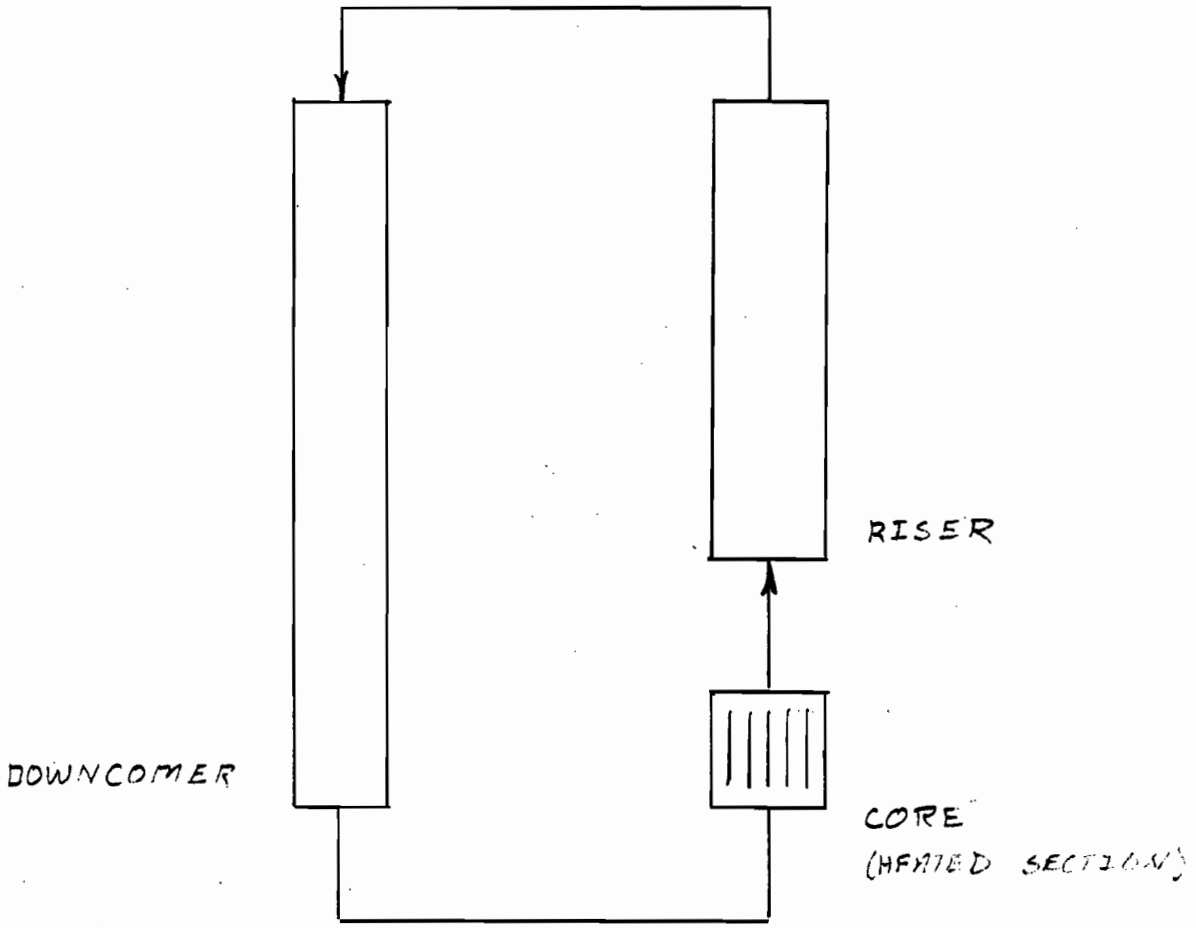

Fig. 1. Piping loop.

The pressure drop along each of the three loop sections can be expressed as the sum of the inertial, acceleration and frictional, and hydrostatic pressure drops (Ref. 2) as:

$$\Delta P = \frac{L}{A}\frac{dW}{dt} + K\frac{W\,|W|}{2\bar{\rho}\,A^2} + \bar{\rho}g\Delta Z \qquad \text{(Eq. 2)}$$

where L = channel length

A = channel cross-sectional flow area

W = mass flow rate in the channel

K = hydraulic loss coefficient expressed in terms of the Darcy-Weisback friction factor f ; K = fL/D

$\bar{\rho}$ = section average water density

g = gravitational constant

ΔZ= channel height.

It should be noted here that the lumped node approach characterized by Eq. 2 is not appropriate for very fast transients, or transients were boiling or rapid depressurization causes rapid changes in fluid density. Substitution of Eq. 2 into Eq. 1 yields:

$$\Delta P = \left[\frac{L}{A}_{core} + \frac{L}{A}_{riser} + \frac{L}{A}_{down}\right]\frac{dW}{dt} + \left[\frac{K}{2\bar{\rho}A^2}_{core} + \frac{K}{2\bar{\rho}A^2}_{riser} + \frac{K}{2\bar{\rho}A^2}_{down}\right]W\,|W|$$

$$+ g\bar{\rho}\Delta Z)_{core} + g\bar{\rho}\Delta Z)_{riser} + g\bar{\rho}\Delta Z)_{down} = 0 \qquad \text{(Eq. 3)}$$

Which is rearranged to yield a first order, ordinary differential equation for system flow rate as a function of time:

$$\frac{dW}{dt} = \frac{-K_T}{\frac{L}{A_T}}\,W\,|W| - \frac{g}{\frac{L}{A_T}}\sum_{1}^{3}\bar{\rho}_i\,\Delta Z_i \qquad \text{(Eq. 4)}$$

where

$$K_T = \frac{K_{core}}{\bar{2}\rho_{core} A^2_{core}} + \frac{K_{riser}}{\bar{2}\rho_{riser} A^2_{riser}} + \frac{K_{down}}{\bar{2}\rho_{down} A^2_{down}}$$

and

$$\frac{L}{A_T} = \frac{L}{A_{core}} + \frac{L}{A_{riser}} + \frac{L}{A_{down}}$$

Accurate evaluation of Eq. 4 requires that one have knowledge of the time and space dependent temperature response of the system in order that accurate estimates of the various density terms can be evaluated. Assuming single phase, incompressible, homogeneous conditions, the energy balance for the heated section is:

$$M_h C_p \frac{dT_h}{dt} = WC_p (T_d - T_h) - HA (T_h - T_s) + Q \qquad \text{(Eq. 5)}$$

which is rearranged to yield:

$$\frac{dT_h}{dt} = \frac{WC_p}{M_h C_p} (T_d - T_h) - \frac{HA}{M_h C_p} (T_h - T_s) + \frac{Q}{M_h C_p} \qquad \text{(Eq. 6)}$$

where

T_h	=	heated section water temperature
W	=	loop flow rate
M_h	=	heated section nodal fluid mass
C_p	=	nodal fluid specific heat
T_d	=	downcomer nodal fluid temperature
H	=	overall heat transfer coefficient from heated section fluid to the environment
A	=	area for heat transfer from heated fluid to environment
T_s	=	environment temperature
Q	=	energy input rate to heated fluid section

The energy balances for the remaining nodes of the system are identical to that for the heated section, except that there is no energy source term (Q) present, i.e.:

$$\frac{dT_i}{dt} = \frac{WC_p}{M_iC_p}(T_{i-1} - T_i) - \frac{HA}{M_iC_p}(T_i - T_{si}) \qquad \text{(Eq. 7)}$$

Equation 7 can be replicated as needed to evaluate systems that have more than one riser or downcomer node.

2.2 Model Implementation

Equations 4, 6, and 7 constitute a set of coupled, first order, ordinary differential equations, which, when supported with the appropriate physical properties routines, can be solved to yield the time dependent system flow rate and fluid temperature in each section of the loop. This approach has been implemented in the NATC model at ORNL. See Appendix A for a brief description of NATC's input data requirements. Simply described, NATC consists of a series of FORTRAN coded routines which read user input, define the differential equations, evaluate the necessary physical properties, calculate the nuclear decay heat rate (for reactor applications), solve the differential equations, and print the results for each time step.

In the present version of NATC, the system is assumed to be subdivided into six nodes or control volumes (Figure 2), i.e. one node for the heated section, one node for the riser section, and four nodes in the return or downcomer section. The present version of the model assumes no heat loss through the walls of the heated and riser sections. Nodes 3 through 6 are, however, assumed to exchange energy via convection with a fixed temperature heat sink. The heat transfer coefficient for each node is a user input value, and there is no explicit treatment of energy storage in the loop walls, internal structures, etc. The user

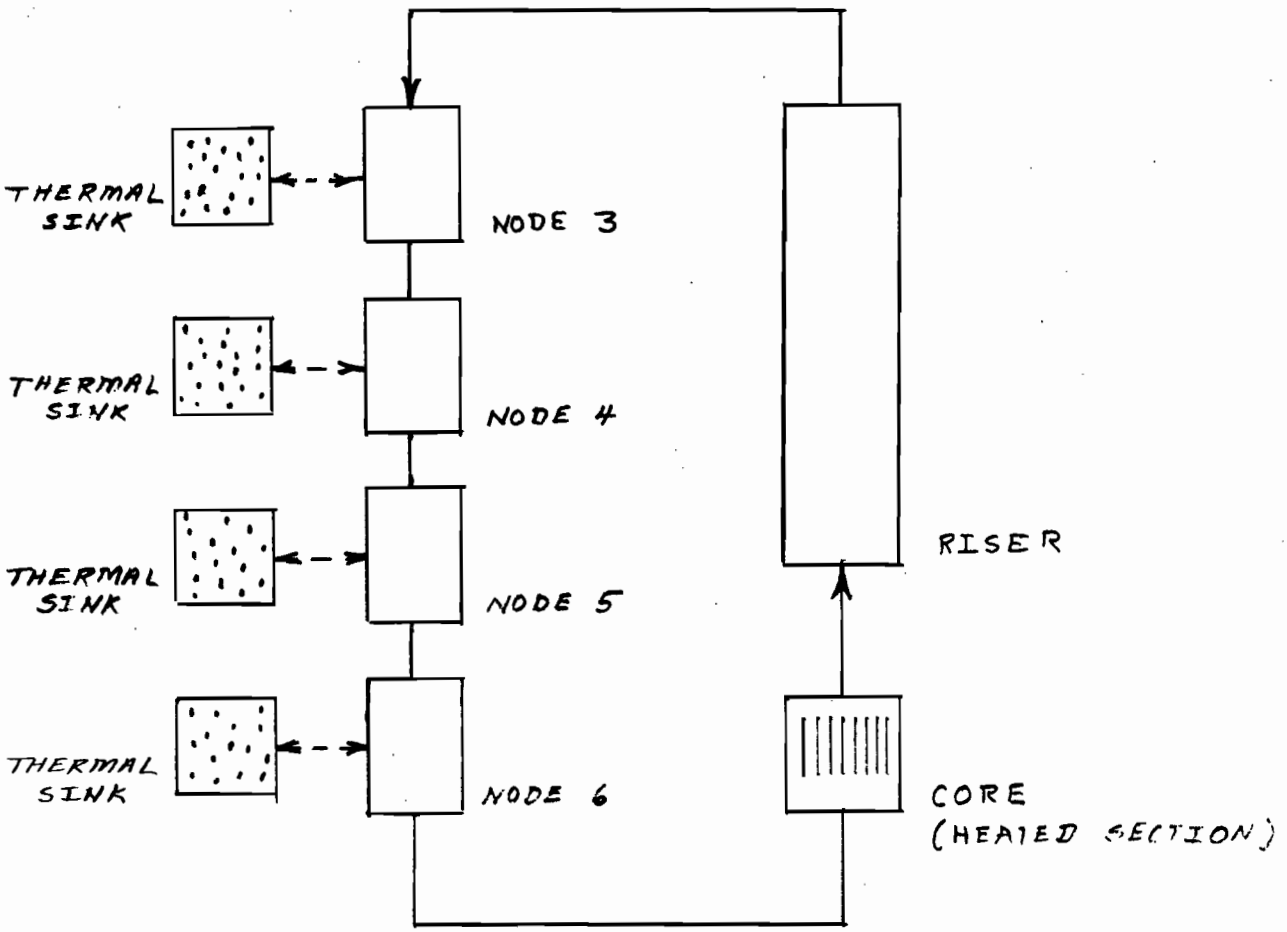

Fig. 2. NATC system configuration.

is given the option of specifying a constant energy source (Q) for the heated section, or employing the ANS 5.1 - 1979 decay heat curve (Ref. 3) for reactor cooling studies. The differential equations employed in NATC are given in Table 1.

NATC employs the LSODE (Ref. 4) differential equation solution package, which was developed at the Lawrence Livermore National Laboratory, and is available on the ORNL computer system. LSODE offers the user a variety of solution techniques which may be applied to both stiff and nonstiff systems and provides a convenient solution method for the analyst who does not desire to encode his own solution algorithm.

3. NATC BENCHMARK STUDY: TVA THERMAL PUMP EXPERIMENT

3.1. Description of Experiment

As part of an on-going effort to evaluate the feasibility of ASEA's PIUS reactor concept (Ref. 5), TVA's Engineering Laboratory at Norris, Tennessee recently performed a series of small scale experiments designed to investigate the fundamental safety and operational principles of the PIUS concept. One of these investigations (Ref. 6) consisted of the construction and testing of a small scale "Thermal Pump" model (Figure 3). As shown in Figure 3, the experimental apparatus was constructed from a 24-inch length of 12-inch diameter piping. The rig was fitted with seven thermocouples located in the positions shown in Figure 3. The thermal energy source was provided by a 639 watt resistive heater which was located in the lower section of the riser. The object of this test was to investigate the nature of the pressure balance concept employed in the PIUS design to separate the hot primary system water from the cooler pool water, and the behavior of the induced natural circulation upon breakdown of the lower interface.

The test was performed in the following manner: (1) the apparatus was filled with tap water, (2) air bubbles were introduced at the top

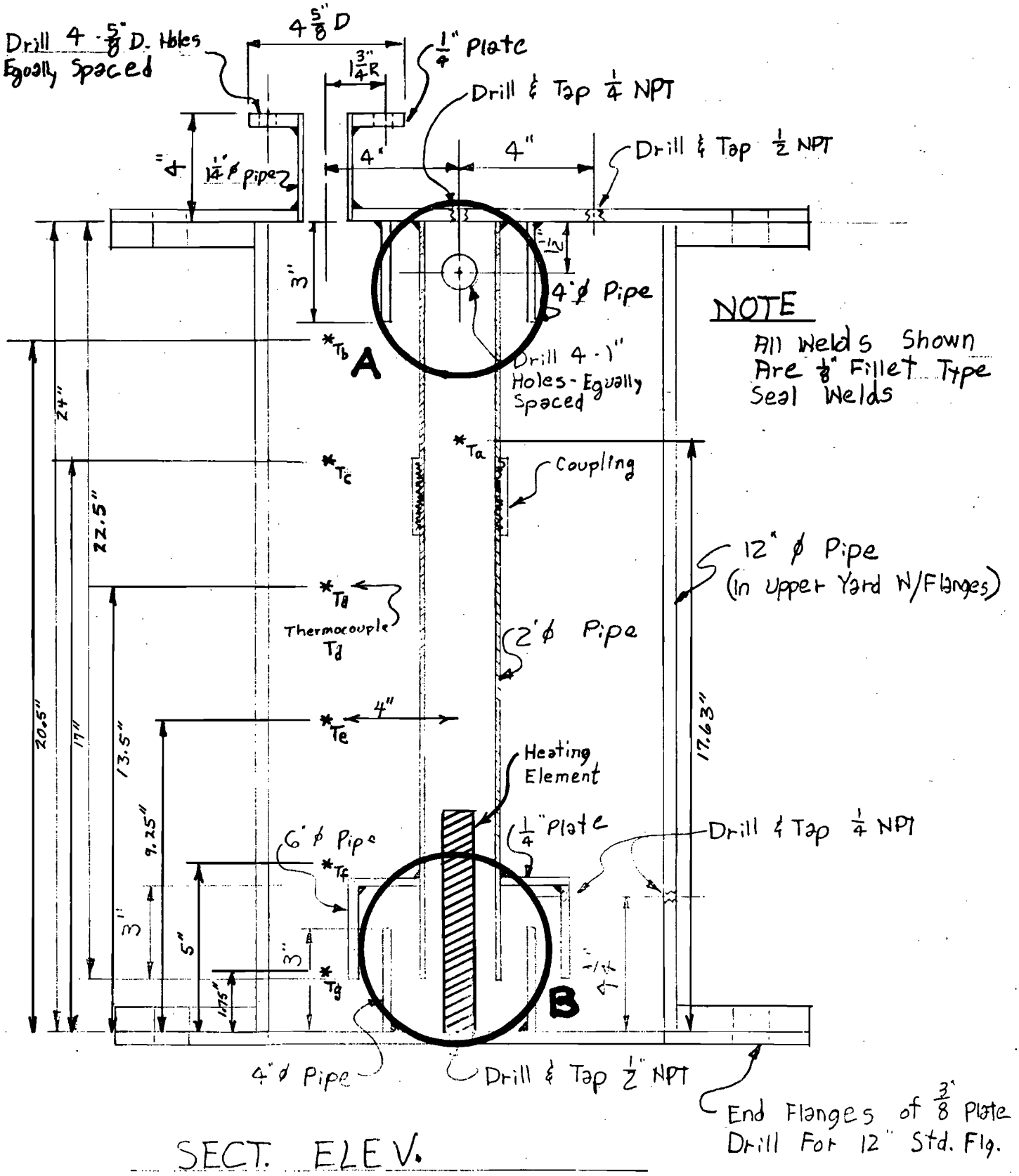

Fig. 3. TVA thermal pump.

and bottom interfaces (regions A and B in Figure 3) to effectively isolate the water in the central 2" riser pipe from the water in the remainder of the pump, (3) the heater was turned on and the riser and pool water temperatures were recorded, (4) when the temperature of the water in the isolated riser section reached 100 degrees Fahrenheit (this occurred at approximately 79 minutes into the test), the two air bubbles were quickly bled off, resulting in the establishment of a natural circulation path by which the heated water circulates up the riser, down through the pool, and back into the riser's heated section, (5) the heater was left on and data were recorded for approximately 80 minutes following initiation of the circulation. The test data gathered from this experiment are presented in Table 2 and plotted in Figures 4 and 5. It should be noted that the data shown in Table 2 has been processed to provide experimental data in a form consistent with the topology of the ORNL model. This was necessary because TVA employed six thermocouplers in the outer zone of the test rig, while the ORNL model topology can accommodate only four modes in that same region. Referring to Table 2 and Figure 3:

$$T_2 = T_a$$
$$T_3 = T_b$$
$$T_4 = (T_c + T_d)/2.$$
$$T_5 = (T_e + T_f)/2.$$
$$T_6 = T_g.$$

3.2 NATC Analysis of Experiment

Following initiation of natural circulation, the thermal pump can be viewed as a closed loop system as depicted in Figure 1. This test, therefore, provides a good benchmark by which the capabilities of NATC can be evaluated. The fundamental NATC input data (presented in Appendix B) were prepared by TVA and provided to ORNL along with the test data previously described (Ref. 6). The reader will note that no

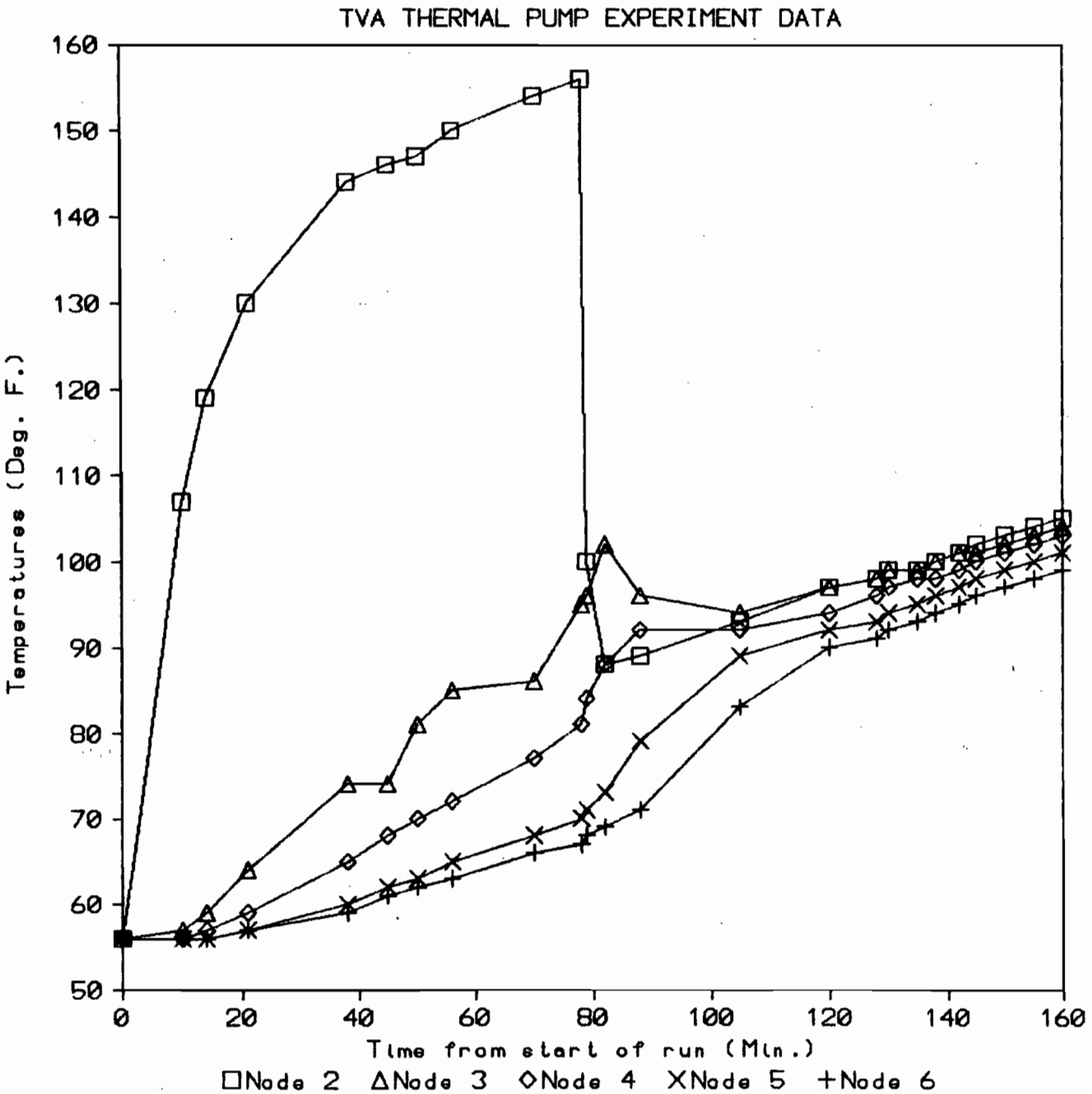

Fig. 4. TVA thermal pump test data.

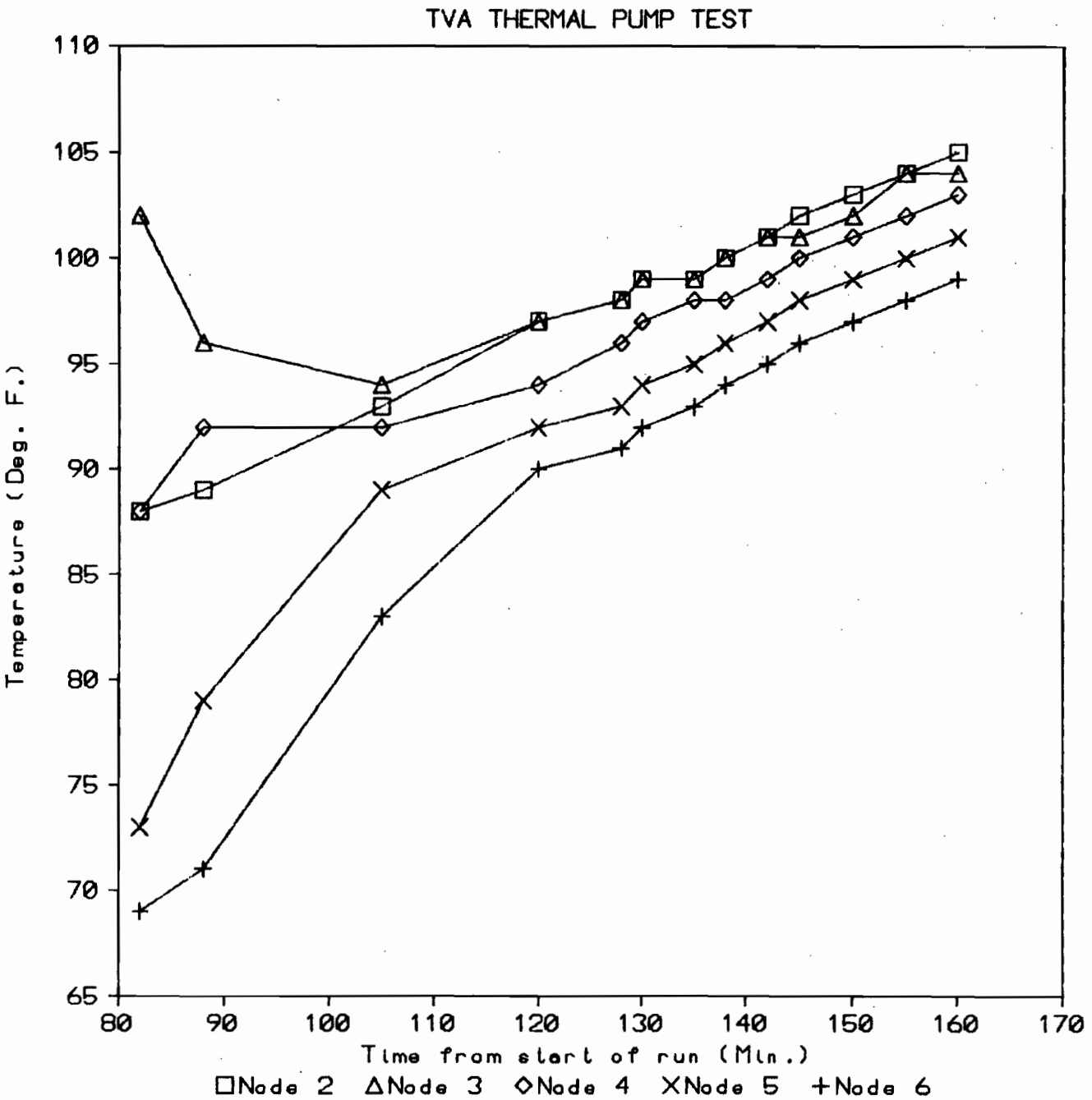

Fig. 5. TVA thermal pump test data — expanded view of 80-160 minute interval.

temperature data were available for the water in the region directly adjacent to the heater element. Since NATC requires initial temperature data for each zone in the loop, the required initial fluid temperature estimate for the heated zone was obtained by equating the temperature to the arithmetic average of the pool bottom and riser temperatures. Four cases were examined. In each case the NATC analysis was initiated at 82 minutes into the test - a time at which the loop's circulatory flow is fully established. This approach was necessary due to NATC's inability to simulate the early, highly dynamic phase of the transient in which the air bubbles are bled off and the initial flow is established. The input assumptions utilized in each case are summarized in Table 3. The results of the analyses are depicted in Figures 6 through 11 and an analysis of the error in the NATC predictions is presented in Tables 4 through 8. It should be noted that NATC results are not available for the entire test period for all four cases due to CPU usage constraints which were imposed on each computer run. The reader will be assisted in interpreting the results of the analysis by referring to Figure 12, which shows the locations of the experimental rig's thermocouples and NATC's homogenized nodes.

As seen from Figures 6-10, the results of all four cases agreed well with the experimental data. In general, Case 1 (the base case) results did not agree as well with the observed temperature trends as did the other three cases. Case 1 provides the worst agreement with the observed responses of every node except the riser - consistently predicting nodal temperatures four to eight degrees in excess of observed values.

For Case 2, the heat transfer coefficients for pool-to-heat sink heat transfer (parameter HXCOEF in the NATC input) were increased by 50-percent for nodes 3 through 6. As one would anticipate, this change resulted in reduction in the predicted temperature of the pool nodes and, in general, much better agreement between the predicted and observed temperatures of all of the nodes.

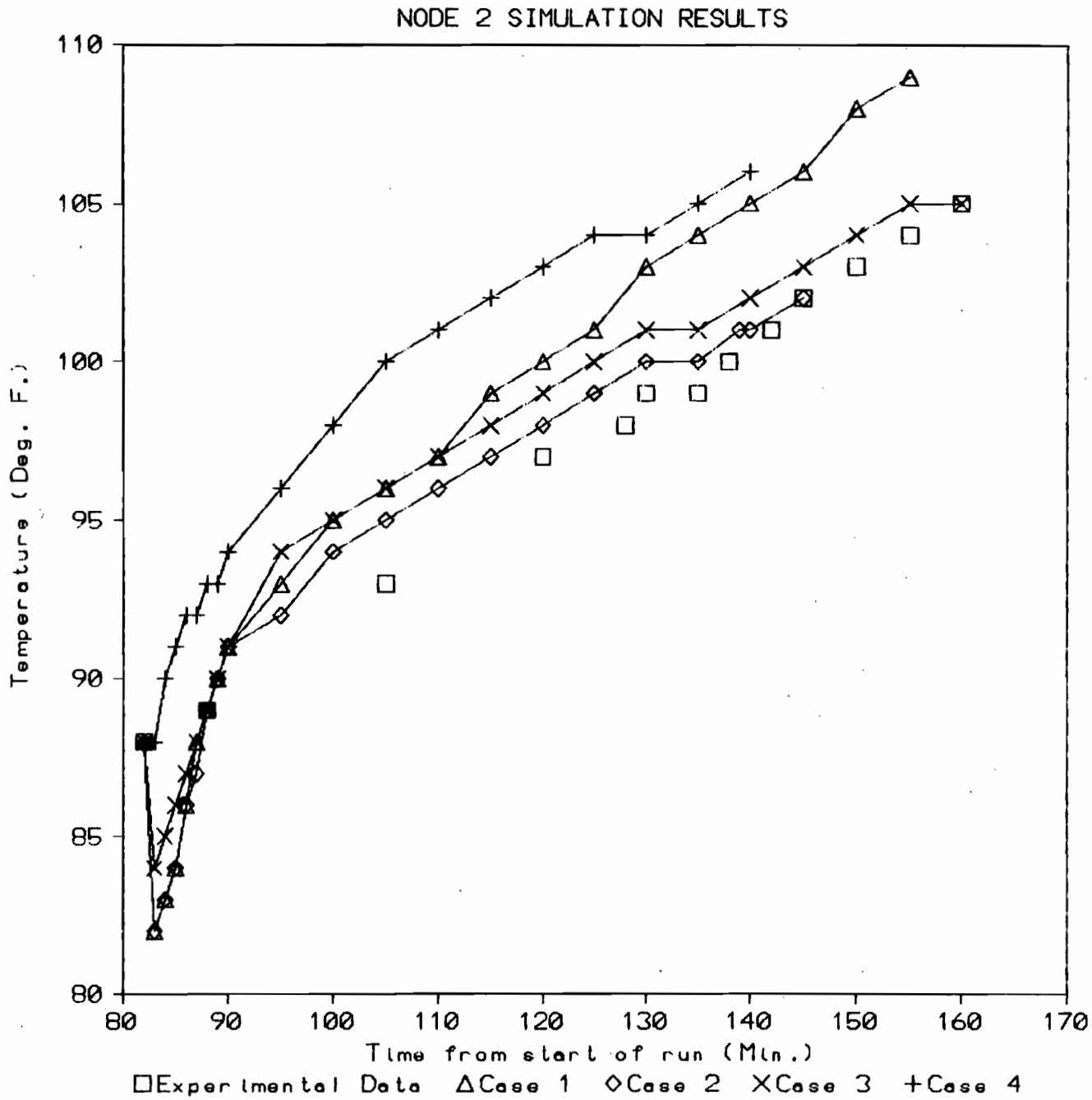

Fig. 6. NATC thermal pump simulation results — Node 2 (riser).

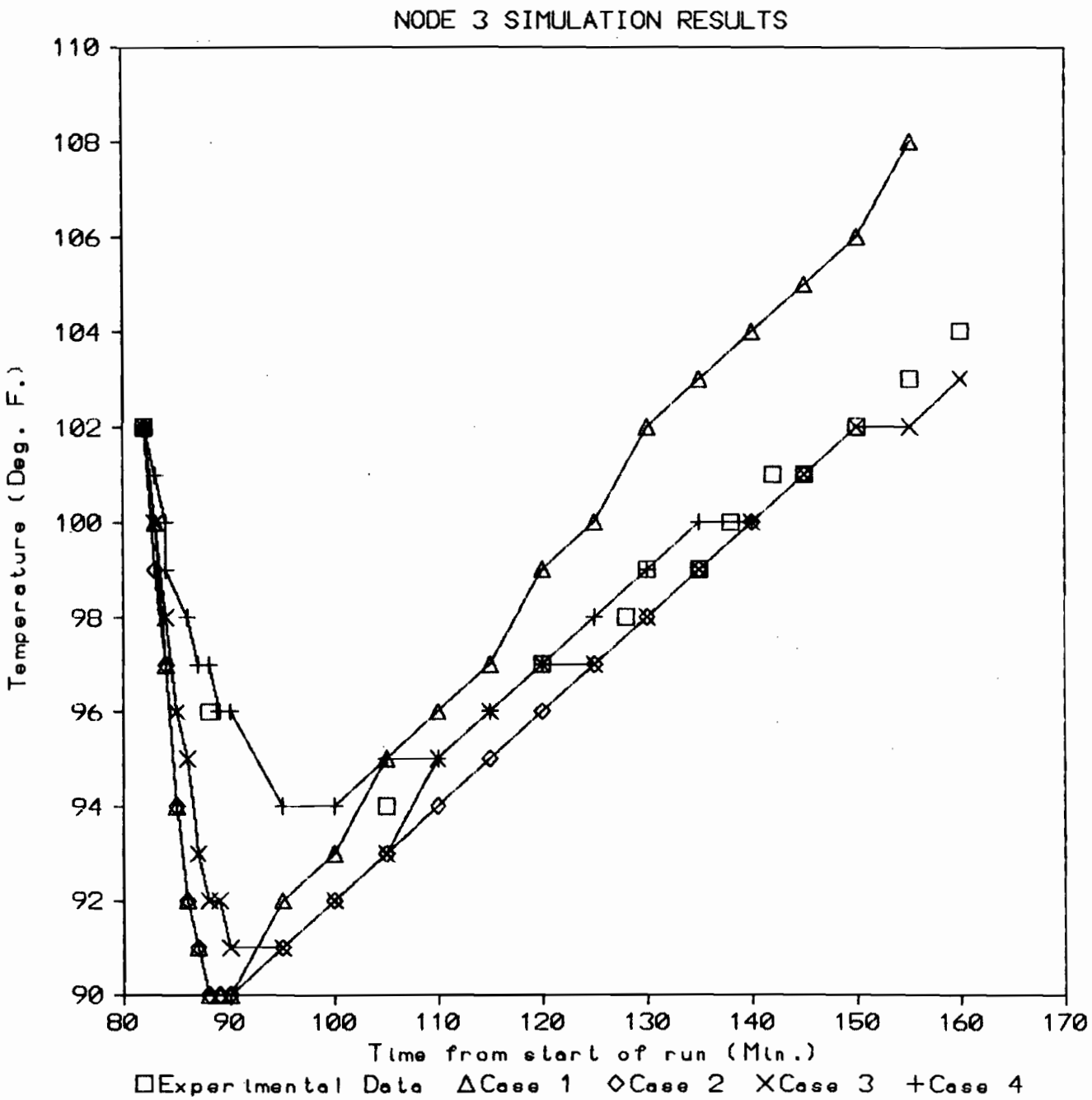

Fig. 7. NATC thermal pump simulation results — Node 3.

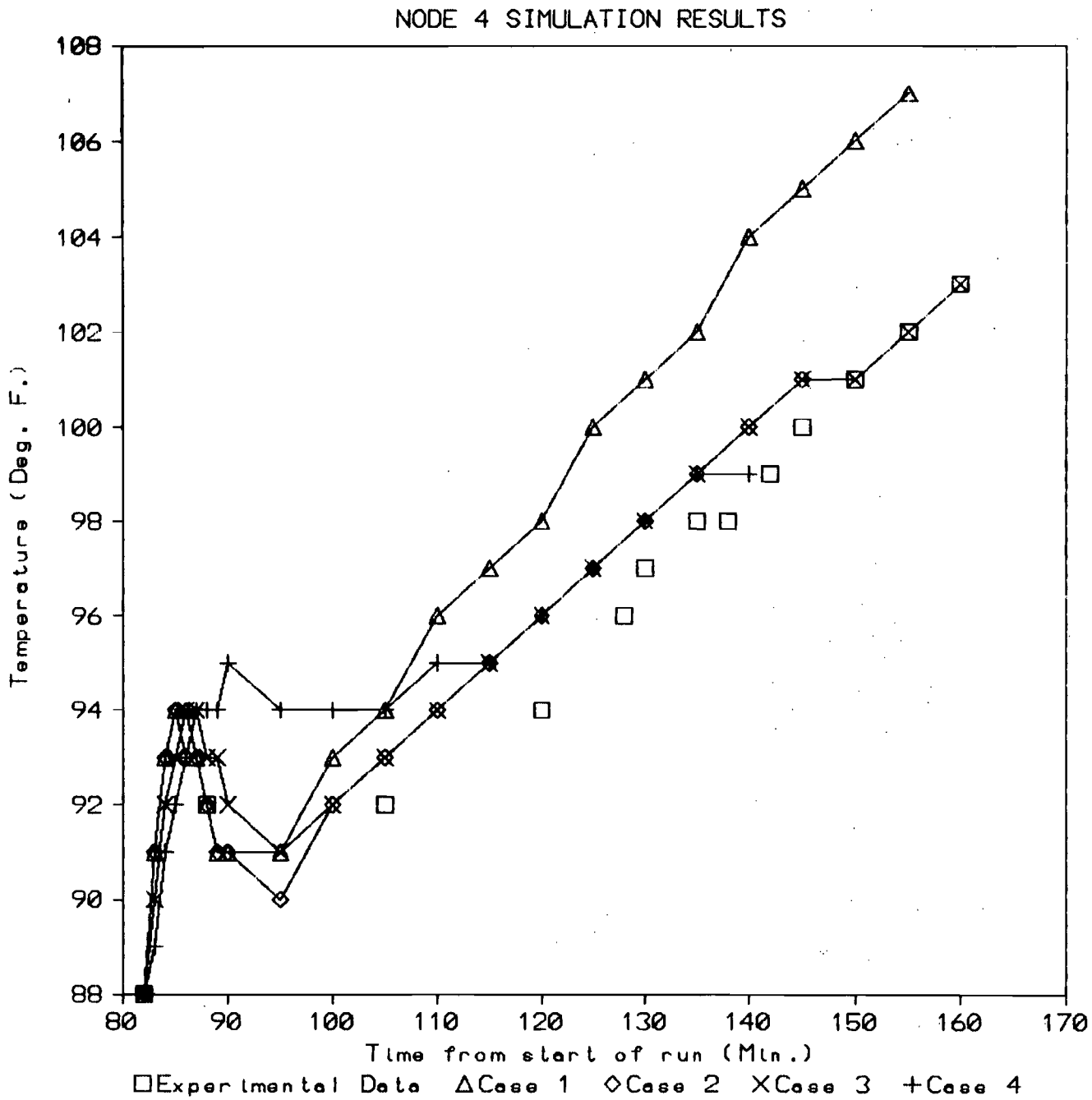

Fig. 8. NATC thermal pump simulation results — Node 4.

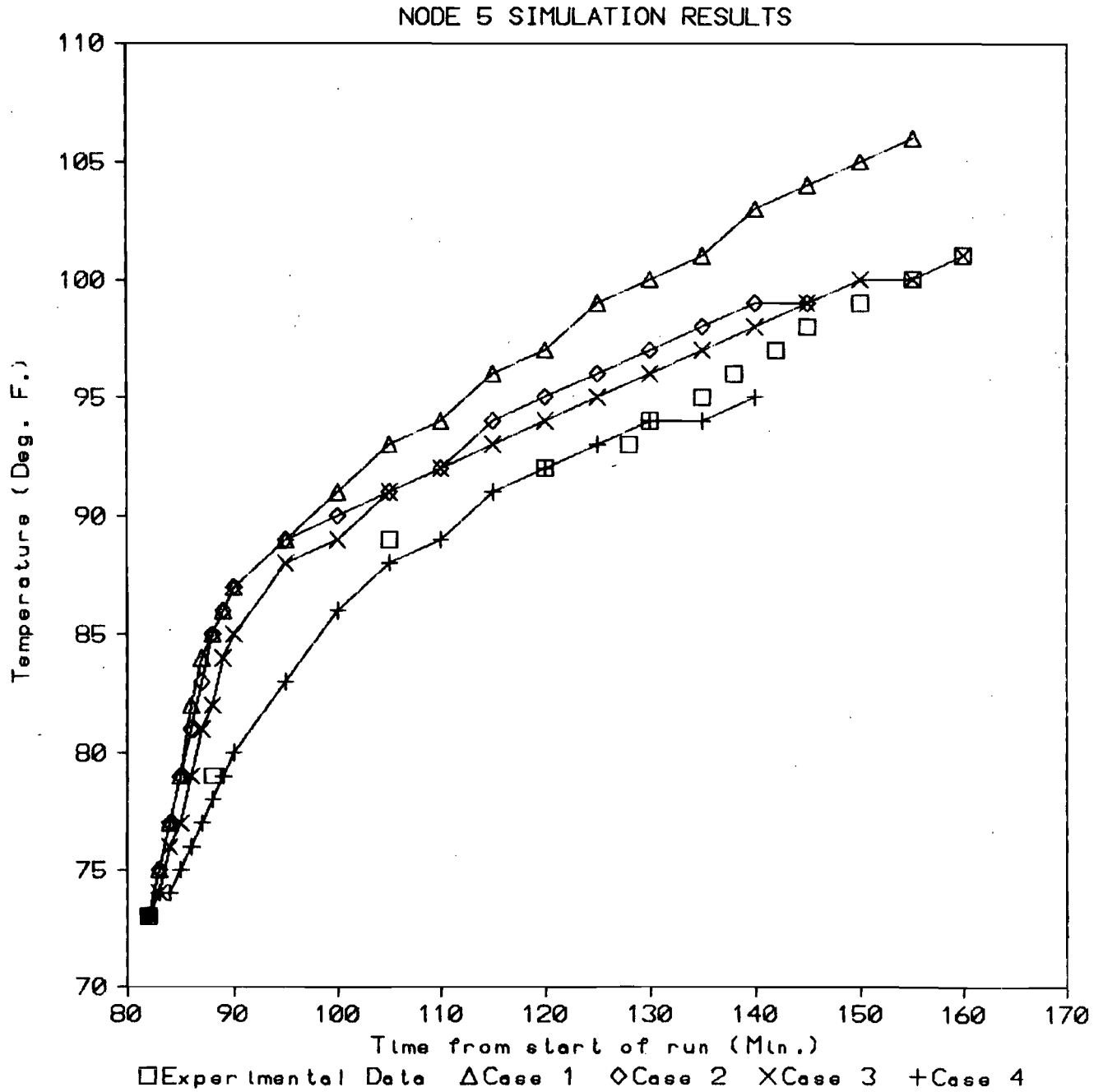

Fig. 9. NATC thermal pump simulation results — Node 5.

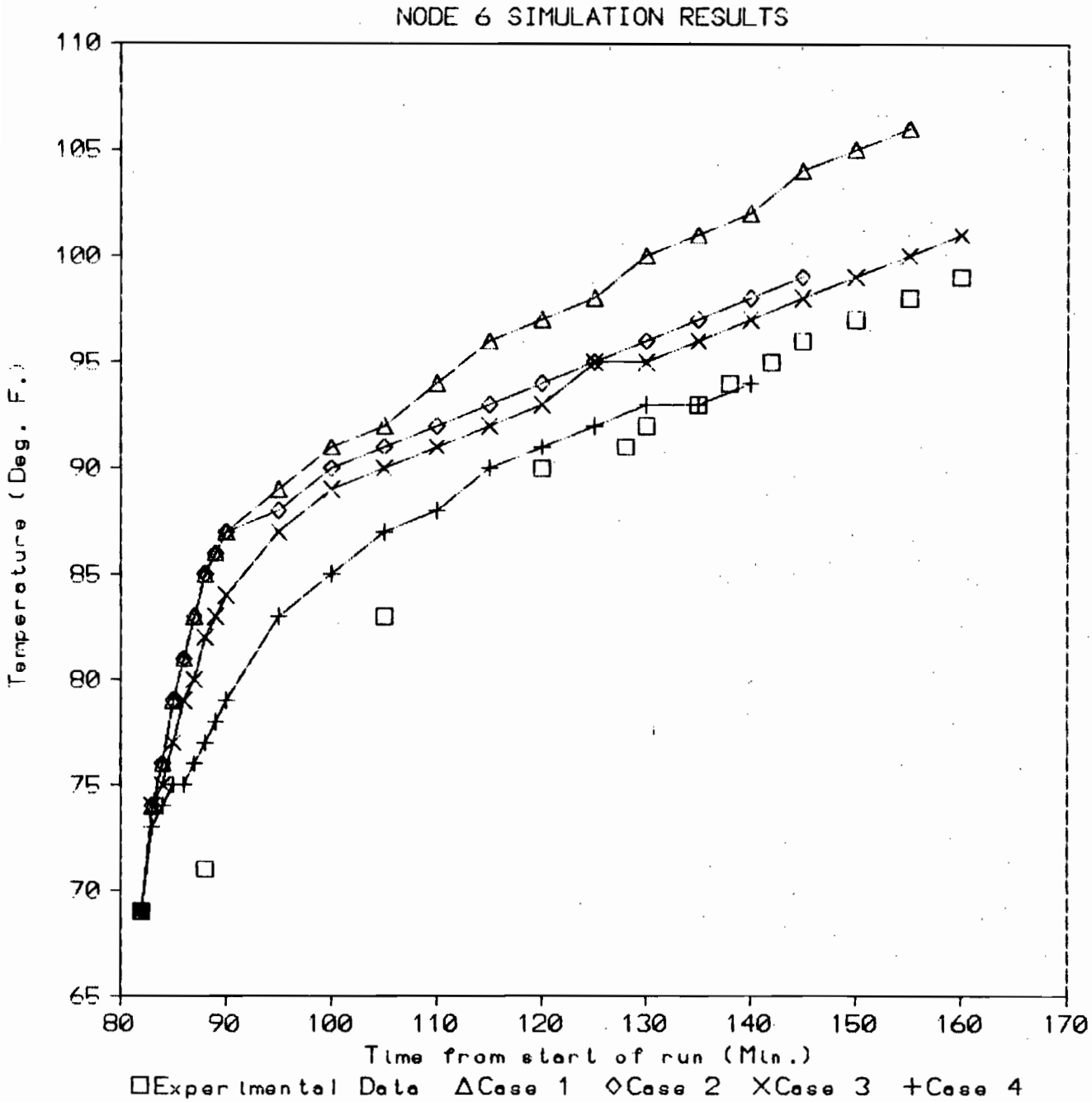

Fig. 10. NATC thermal pump simulation results — Node 6.

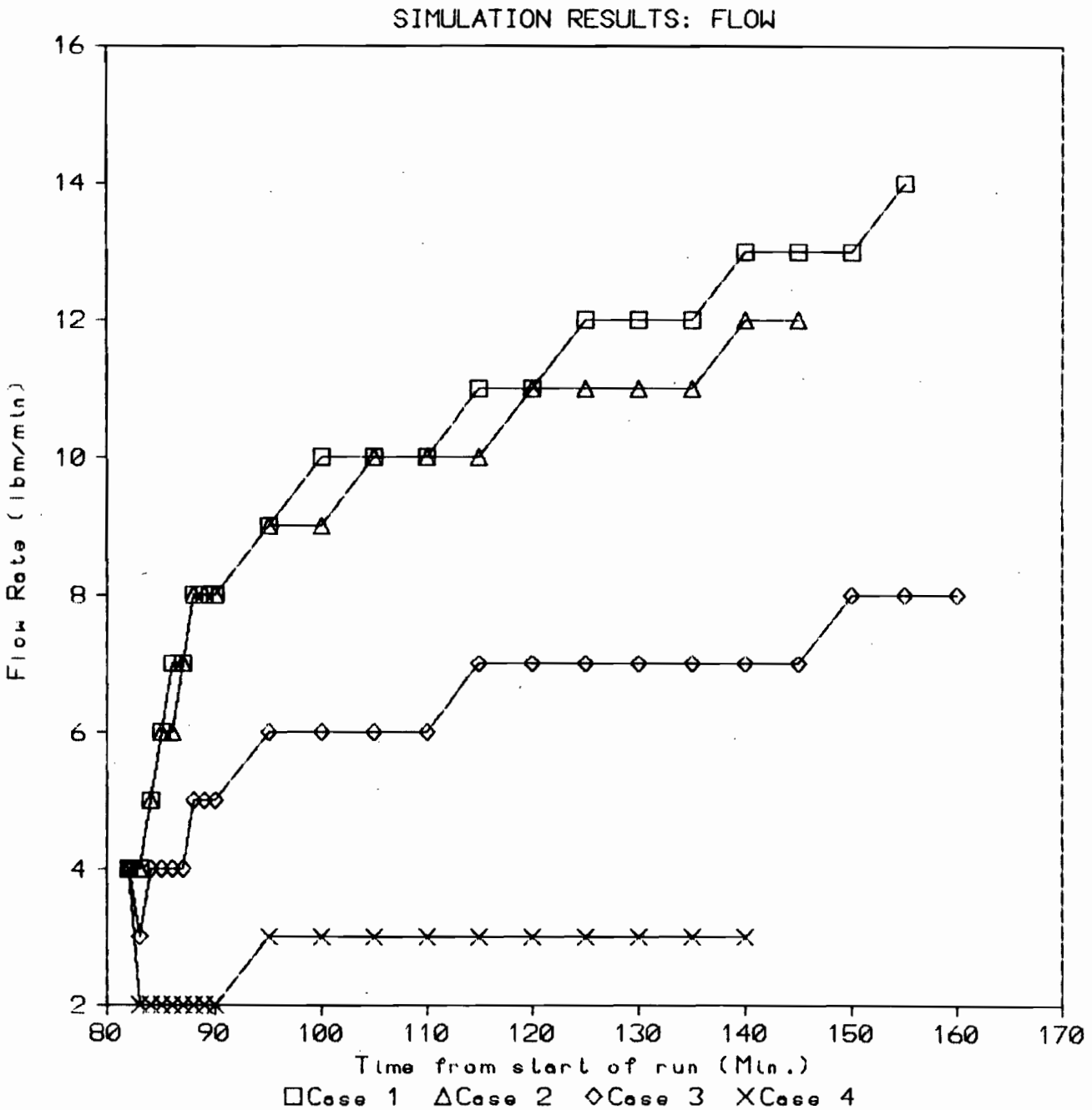

Fig. 11. NATC thermal pump simulation results — flow rate (rounded to the nearest integer lb/min).

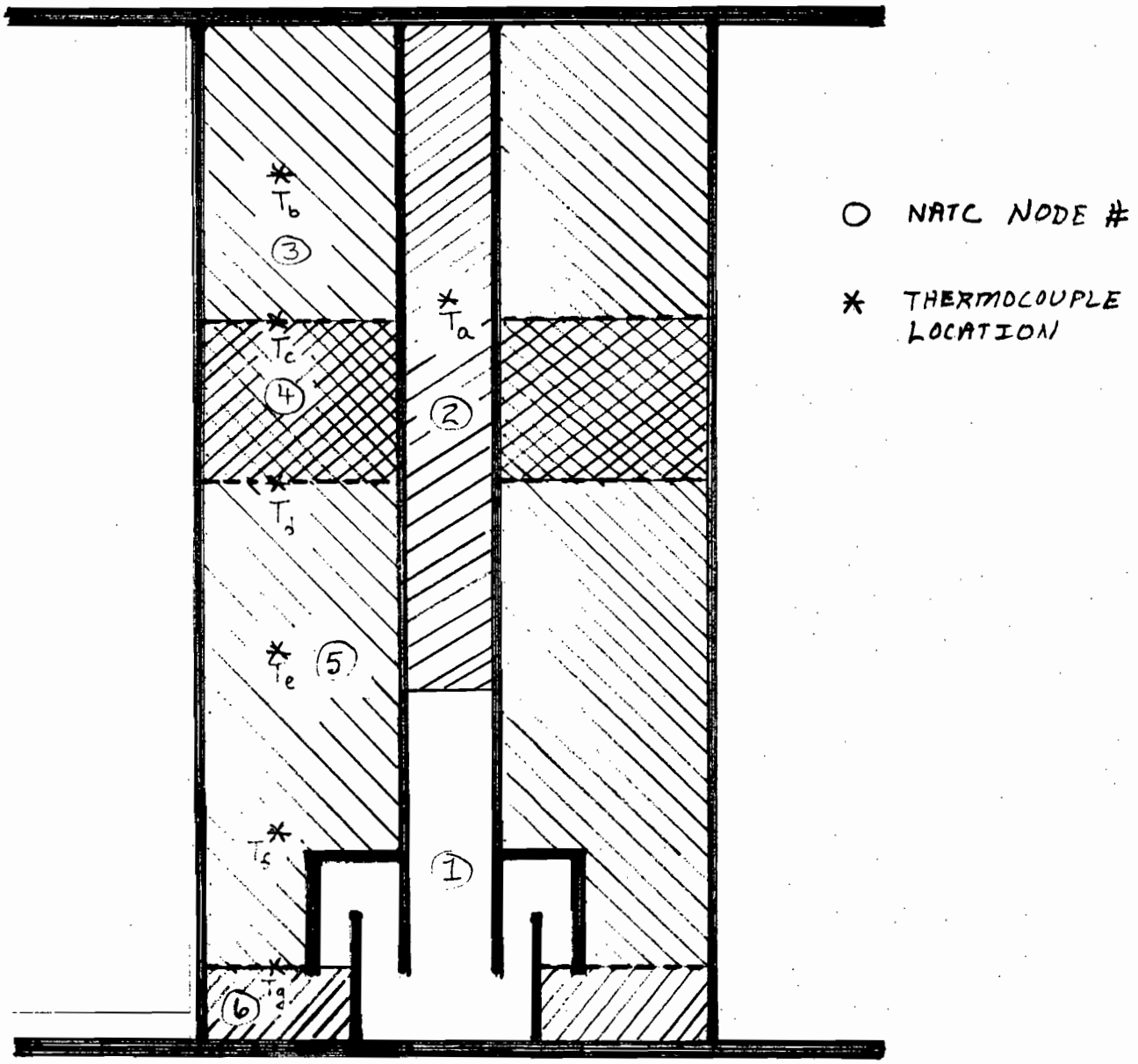

Fig. 12. NATC model noding and experimental temperature measurement points.

For Case 3, the core hydraulic loss coefficient was doubled, while the loop hydraulic loss was tripled. Compared to Case 2 predictions, Case 3 results show a slightly improved agreement with the observed temperatures of (downcomer) nodes 3 thorough 6, and a slightly poorer agreement with the observed temperatures of node 2 (the riser).

In the final case, Case 4, the core hydraulic loss coefficient was increased again, by a factor of 15.43, while the loop hydraulic loss coefficient was increased by a factor of 16.75. (These numbers result from the arbitrary decision to set $K_{core} = 50$ and $K_{loop} = 100$.) The results of this case provided the best fit to the observed temperatures of nodes 5 and 6, and the worst fit to the observed temperature of node 2 (the riser).

Figure 11 displays the NATC predictions for loop flow rate as a function of time for each of the four cases previously discussed. As expected, Cases 3 and 4 result in significantly lower predicted flow rates than Cases 1 and 2. It is interesting to note that the predicted flow rates for Case 2 are slightly lower than those for Case 1. It is not clear at this time why this is so, but the increased heat transfer coefficient in the downcomer cells in Case 2 appears to be leading to slightly decreased density head differences in the two vertical fluid columns (recall that the data in Figure 11 are rounded to the nearest 1 lb/min). It is possible that the observed phenomenon is a result of small irregularities in the density vs. temperature data in the physical properties routines.

4. CONCLUSIONS

A simple dynamic model for analysis of a single phase, water cooled, natural convection systems has been developed and benchmarked against data from a recent experiment performed by TVA. An analysis of Tables 4 through 8 leads to the following observations and conclusions:

1. In general, the NATC modeling approach provides a relatively simple, but credible tool for the analysis of single phase, natural convection heat transfer in loop-type systems. The predictive accuracy of NATC is sufficient to provide a useful working tool for evaluation of differing system configurations and for development of an integrated understanding of the behavior of such systems;

2. The accuracy of the NATC results is poorest for those nodes which have the largest structural surface area-to-water mass ratio. It is believed that this error is primarily due to the absence of a fluid-to-internal structure heat transfer model in NATC (i.e. the heat capacity of internal structures is ignored). This conclusion is supported by an analysis of Table 9, which indicates that nodes 2 and 6 have the largest structural heat transfer area-to-water mass ratio, and Tables 4 through 8, which indicate that the error in NATC predictions is largest for these two nodes;

3. Although the accuracy of the NATC results for many applications is acceptable, relatively simple model improvements could result in a significant improvement in NATC modeling accuracy, i.e.

a. incorporation of a model for heat transfer between the fluid and internal structures within each node

b. incorporation of suitable heat transfer coefficient correlations;

4. The NATC modeling approach is amenable to application to single loop systems with pumps by the addition of a pump head term in Equation 4, i.e.;

$$\frac{dW}{dt} = \frac{-K_T}{\frac{L}{A_T}} W \, |W| - \frac{g}{\frac{L}{A_T}} \sum_{1}^{3} \bar{\rho}_i \, \Delta Z_i + \bar{\rho} \, g \, H_p(t)$$

where $\bar{\rho}$ = average fluid density of water being pumped
$H_p(t)$ = pump head (units of length);

5. NATC could provide a simple, yet useful tool for analysis of reactors such as ASEA's PIUS concept, which rely upon single phase natural convection to remove decay heat from the core.

References

1. E. E. Lewis, Nuclear Power Reactor Safety, John Wiley & Sons, 1977.

2. Ibid, Eq. 7-30.

3. "Decay Heat Power In Light Water Reactors," American Nuclear Society and the American National Standards Institute, ANSI/ANS-5.1-1979, 1979.

4. Alan C. Hindmarsh, "LSODE and LSODI, Two New Initial Value Ordinary Differential Equation Solvers," ACM-SIGNUM Newsletter, Vol. 15, No. 4 (1980).

5. "SECURE-P Design Progress Information," ASEA-ATOM, April 1984.

6. Letter from S. Viegander, Tennessee Valley Authority to S. R. Greene, Oak Ridge National Laboratory, February 14, 1985.

Table 1. NATC Equations

$$\frac{dW}{dT} = \frac{-K_T}{\frac{L}{A_T}} W |W| - \frac{g}{\frac{L}{A_T}} \sum_{1}^{6} \bar{\rho}_i \Delta Z_i$$

$$\frac{dT_c}{dt} = \frac{WC_p}{M_c C_p} (T_6 - T_c) + \frac{Q}{M_c C_p}$$

$$\frac{dT_R}{dt} = \frac{WC_p}{M_R C_p} (T_c - T_r)$$

$$\frac{dT_3}{dt} = \frac{WC_p}{M_3 C_p} (T_r - T_3) - \frac{HA}{M_3 C_p} (T_3 - T_s)$$

$$\frac{dT_4}{dt} = \frac{WC_p}{M_4 C_p} (T_3 - T_4) - \frac{HA}{M_4 C_p} (T_4 - T_s)$$

$$\frac{dT_5}{dt} = \frac{WC_p}{M_5 C_p} (T_4 - T_5) - \frac{HA}{M_5 C_p} (T_5 - T_s)$$

$$\frac{dT_6}{dt} = \frac{WC_p}{M_6 C_p} (T_5 - T_6) - \frac{HA}{M_6 C_p} (T_6 - T_s)$$

Table 2. TVA thermal pump experimental data
(Small Pipe Test No. 16)

Nodal Temperatures (°F)*

Time	T_1	T_2	T_3	T_4	T_5	T_6
0		56	56	56	56	56
10	-	107	57	56	56	56
14	-	119	59	57	56	56
21	-	130	64	59	57	57
38	-	144	74	65	60	59
45	-	146	79	68	62	61
50	-	147	81	70	63	62
56	-	150	85	72	65	63
70	-	154	86	77	68	66
78	-	156	95	81	70	67
79	-	100	96	84	71	68
82	-	88	102	88	73	69
88	-	89	96	92	79	71
105	-	93	94	92	89	83
120	-	97	97	94	92	90
128	-	98	98	96	93	91
130	-	99	99	97	94	92
135	-	99	99	98	95	93
138	-	100	100	98	96	94
142	-	101	101	99	97	95
145	-	102	101	100	98	96
150	-	103	102	101	99	97
155	-	104	103	102	100	98
160	-	105	104	103	101	99

*See text page 10

Table 3. Thermal pump study case assumptions

Case 1:	Base case: all input data as supplied by TVA with initial heated section fluid temperature set equal to arithmetic average of initial riser and lowest pool node temperatures
Case 2:	Input data same as Case 1 except heat transfer coefficients for pool-to-heat sink heat transfer (parameter HXCOEF in input) increased by 50% for all pool nodes
Case 3:	Input data same as Case 2 except core hydraulic loss coefficient doubled and loop hydraulic loss coefficient tripled
Case 4:	Input data same as Case 2 except core hydraulic loss coefficient multiplied by 15.43 and loop hydraulic loss coefficient multiplied by 16.75

Table 4. Error analysis for Node 2 NATC predictions

TIME (MIN)	OBS (°F)	NATC Prediction Error (°F)			
		Case 1	Case 2	Case 3	Case 4
82	88	0	0	0	0
88	89	0	0	0	+4
105	93	+3	+2	+3	+7
120	97	+3	+1	+2	+6
128	98	+4	+1	+2	+6
130	99	+4	+1	+2	+5
135	99	+5	+1	+2	+6
138	100	+5	+1	+2	
142	101	+5	+1	+2	
145	102	+4	0	+1	
150	103	+5		+1	
155	104	+5		+1	
160	105			0	

Table 5. Error analysis for Node 3 NATC predictions

TIME (MIN)	OBS (°F)	NATC Prediction Error (°F)			
		Case 1	Case 2	Case 3	Case 4
82	102	0	0	0	0
88	96	-6	-6	-4	+1
105	94	+1	-1	-1	+1
120	97	+2	-1	0	0
128	98	+3	0	0	+1
130	99	+3	-1	-1	0
135	99	+4	0	0	+1
138	100	+4	0	0	0
142	101	+4	-1	-1	
145	101	+4	0	0	
150	102	+4		0	
155	103	+5		-1	
160	104			0	

Table 6. Error analysis for Node 4 NATC predictions

TIME (MIN)	OBS (°F)	NATC Prediction Error (°F)			
		Case 1	Case 2	Case 3	Case 4
82	88	0	0	0	0
88	92	0	0	+1	+2
105	92	+2	+1	+1	+2
120	94	+4	+2	+2	+2
128	96	+5	+2	+2	+2
130	97	+4	+1	+1	+1
135	98	+4	+1	+1	+1
138	98	+5	+1	+1	+1
142	99	+5	+1	+1	
145	100	+5	+1	+1	
150	101	+5		0	
155	102	+5		0	
160	103			0	

Table 7. Error analysis for Node 5 NATC predictions

TIME (MIN)	OBS (°F)	NATC Prediction Error (°F)			
		Case 1	Case 2	Case 3	Case 4
82	73	0	0	0	0
88	79	+6	+6	+3	[illegible]
105	89	+4	+2	+2	-1
120	92	+5	+3	+2	0
128	93	+6	+3	+3	0
130	94	+6	+3	+2	0
135	95	+6	+3	+2	-1
138	96	+6	+2	+1	-1
142	97	+6	+2	+1	
145	98	+6	+1	+1	
150	99	+6		+1	
155	100	+6		0	
160	101			+1	

Table 8. Error analysis for Node 6 NATC predictions

TIME (MIN)	OBS (°F)	NATC Prediction Error (°F)			
		Case 1	Case 2	Case 3	Case 4
82	69	0	0	0	0
88	71	+14	+14	+11	+6
105	83	+9	+8	+7	+4
120	90	+7	+4	+3	+1
128	91	+8	+5	+4	+1
130	92	+8	+4	+3	+1
135	93	+8	+4	+3	0
138	94	+8	+4	+3	0
142	95	+8	+4	+3	
145	96	+8	+3	+2	
150	97	+8		+2	
155	98	+8		+2	
160	99			+2	

Table 9. NATC thermal pump model - nodal characteristics

Node	(M) Water Mass (lbm)	(A) Surface Area (in^2)	A/M (in^2/lbm)
2	1.8	98.0	54.4
3	27.4	402.1	14.7
4	13.7	131.9	9.6
5	33.4	499.1	14.9
6	0.7	188.5	269.3

APPENDIX A

NATC Input Data Description

NATC is currently structured as shown in Figure A.1, with four fluid nodes (or control volumes) in the pool, one in the core, and one in the riser. The following input data are required:

ZTOP(I) The elevation of the top of each control volume (in feet) above the pool bottom. The top of the riser volume, ZTOP(2), is also assumed to be the top of the uppermost pool node, ZTOP(3).

ZBOT(I) The elevation of the bottom of each control volume (in feet) above the pool bottom. The bottom of the core volume, ZBOT(1), is also assumed to be the bottom of the lowest pool volume, ZBOT(6). ZBOT(1) and ZBOT(6) are normally set equal to zero.

SAREA(I) The surface area (square feet) for heat transfer to the pool node. (Zero for the core and riser nodes.) The appropriate areas of the top and bottom of the thermal pump model should be included in SAREA(3) and SAREA(6), respectively.

TEMP(I) The initial temperatures (degrees F) of the fluid in each of the control volumes.

XAREA(I) The cross sectional flow area (square feet) for each control volume.

HXCOEF(I) The nodal heat transfer coefficient (fluid-to-heat sink) in each of the pool nodes. HXCOEF(1) = HXCOEF(2) = 0. (units of Btu/hr ft^2F)

TSINK The heat sink temperature (in degrees F) - currently assumed to be the same for all pool nodes.

FKCORE The hydraulic loss coefficient for the core (heated) node, expressed in inverse square feet;

> FKCORE = (Core pressure drop) *2* (core coolant density)* (core cross-sectional flow area squared) / (flow rate squared) or, = standard hydraulic loss coefficient (K=fL/D) divided by characteristic cross sectional flow area (XAREA).

ATCORE Core node cross-sectional flow area, expressed in square feet.

FLOAC The core height-to-cross-sectional flow area ratio, expressed in inverse feet.

FKLOOP	The riser/pool hydraulic loss coefficient, expressed in inverse square feet. See FKCORE for definition.
ATLOOP	Riser/pool cross-sectional flow area, expressed in square feet.
FLOAL	The riser/pool loop length-to-cross-sectional flow area ratio, expressed in inverse feet.

Additional input data required are the start time for the transient, and a time history of the heater power input for the transient of interest. Due to the design of the mathematical model, all analyses must begin subsequent to initiation of loop flow.

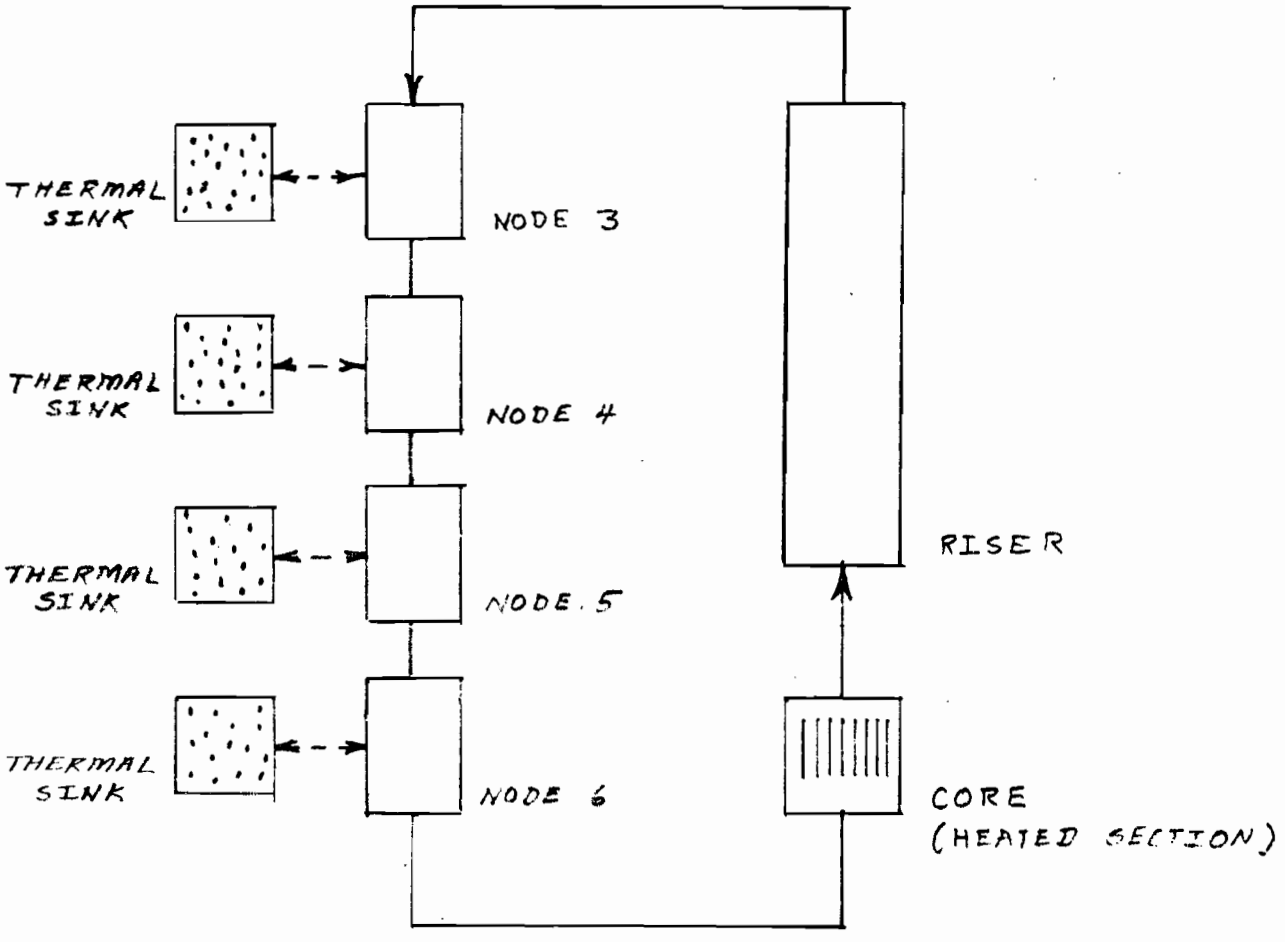

Fig. A.1. NATC model configuration.

APPENDIX B:

NATC Thermal Pump Model Input Data Provided by TVA

A. Node Top Elevation, feet above pool bottom
   1. 0.700
   2. 2.000
   3. 2.000
   4. 1.416
   5. 1.124
   6. 0.146

B. Node Bottom Elevation, feet above pool bottom
   1. 0.000
   2. 0.700
   3. 1.416
   4. 1.124
   5. 0.146
   6. 0.000

C. Node Inside Surface Area, ft^2 (fluid to liner)
   1. 0.00
   2. 0.00
   3. 2.33
   4. 0.82
   5. 2.76
   6. 1.09

D. Initial Water Temperature
   65°F (all nodes)

E. Node Cross-Sectional Flow Area, ft^2
   1. (see I)
   2. (see L)
   3. 0.7546
   4. 0.7546
   5. 0.5460
   6. 0.0777

F. Node Heat Transfer Coefficient, Btu/(hr ft^2 F) fluid to heat sink
   1. 0.000
   2. 0.000
   3. 5.516
   4. 1.033
   5. 3.450
   6. 3.946

G. Heat Sink Temperature
   67°F

H. Core Hydraulic Loss Coefficient
$3.24/ft^2$

I. Core Cross-Sectional Flow Area
$0.0212\ ft^2$

J. Core Height/Cross-Sectional Flow Area
33.019/ft

K. Riser Hydraulic Loss Coefficient
$5.97/ft^2$

L. Riser Cross-Sectional Flow Area
$0.0218\ ft^2$

M. Riser Height/Cross-Sectional Flow Area
59.633/ft

N. Start Time for Transient
78 minutes

O. Heater Input
2174 Btu/hr

P. Air Volume in Airlocks, ft^3

Node	Before Transient	After Transient
2	0.006	0.002
3	0.014	0.058
5	0.040	0.000

APPENDIX C:

Example NATC Input Data File

```
**** TSO FOREGROUND HARDCOPY ****
DSNAME=SRG.TVA6.DAT

 TVA THERMAL PUMP SIMULATION -- CASE 6, (CASE 3 + INCREASED FLOAC & FLOAL)
 &NLSODE
    NEQ = 7,
    TZERO = 82.,
    TSTEP = 1.,
    TSTOP = 160.,
    ITOL = 1,
    RTOL = 1.E-06,
    ATOL = 1.E-06,
    ITASK = 1,
    ISTATE = 1,
    IOPT = 1,
    LRW = 150,
    LIW = 50,
    MF = 22,
 &END
 &NLOPT
    IPROP = 1,
 &END
 &NLNODE
    NUMNOD=6,
    ZTOP(1) = 0.700,  2.000,  2.000,  1.416,  1.124,  0.146,
    ZBOT(1) =  0.,  0.700,  1.416,  1.124,  0.146,  0.,
    XAREA(1) = 0.0212,  0.0218,  0.7546,  0.7546,  0.5460,  0.0777,
    SAREA(1) = 2*0.,  2.33,  0.82,  2.76,  1.09,
    FXCOEF(1) = 2*0., 8.274,  1.549,  5.175,  5.919,
    THICK(1) = 6*0.,
    TEMPI(1) = 78.5,  88.,  102.,  88.,  73.,  69.,
    TSINK = 67.,
 &END
 &NLCORE
    FKCORE = 3.24,
    ATCORE = 0.0212,
    POWER = 36.23,
    FLOAC = 330.,
 &END
 &NLLOOP
    FKLOOP = 5.97,
    ATLOOP = 0.0218,
    FLOAL = 596.,
 &END
```

DISTRIBUTION

1. S. J. Ball
2. J. C. Cleveland
3. T. E. Cole
4. W. G. Craddick
5-8. S. R. Greene
9. J. E. Jones Jr.
10. P. R. Kasten
11. D. L. Moses
12. H. E. Trammell
13. D. B. Trauger
14. J. D. White
15. ORNL Patent Office
16-18. Laboratory Records Department
19. Laboratory Records, RC